Accepted Manuscript

Factors governing the adsorption of ethanol on spherical activated carbons

A.J. Romero-Anaya, M.A. Lillo-Ródenas, A. Linares-Solano

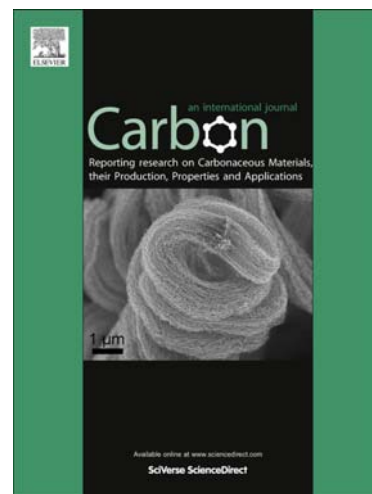# FACTORS GOVERNING THE ADSORPTION OF ETHANOL ON SPHERICAL

ACTIVATED CARBONS

A.J. Romero-Anaya[1], M.A. Lillo-Ródenas, A. Linares-Solano

Departamento de Química Inorgánica, Universidad de Alicante, Ap. Correos 99. E-03080, Alicante, Spain

---

[1] Corresponding author. Fax: +34 965903454. E-mail address: ajromero@ua.es (A.J. Romero-Anaya)

ABSTRACTS

Ethanol adsorption on different activated carbons (mostly spherical ones) was investigated covering the relative pressure range from 0.001 to 1. Oxygen surface contents of the ACs were modified by oxidation (in HNO_3 solution or air) and/or by thermal treatment in N_2. To differentiate the concomitant effects of porosity and oxygen surface chemistry on ethanol adsorption, different sets of samples were used to analyse different relative pressure ranges (below 1000 ppmv concentration and close to unity). To see the effect of oxygen surface chemistry, selected samples having similar porosity but different oxygen contents were studied in the low relative pressure range. At low ethanol concentration (225 ppmv) adsorption is favoured in oxidized samples, remarking the effect of the oxidizing treatment used (HNO_3 is more effective than air) and the type of oxygen functionalities created (carboxyl and anhydride groups are more effective than phenolic, carbonyl and derivatives). To analyse the high relative pressure range, spherical and additional ACs were used. As the relative pressure of ethanol increases, the effect of oxygen-containing surface groups decreases and microporosity becomes the most important variable affecting the adsorption of ethanol.

1. Introduction.

Ethanol, a polar volatile organic compound (VOC), has been raising a lot of interest in recent years because of its applications as biofuel or as an additive to gasoline [1,2,3,4]. Due to this, global production of ethanol from different agroindustrial residues has increased continuously, from 17 billion liters in 2000 [5], to over 86 billion liters in 2011 [6]. Ethanol, in addition to be an additive to improve fuel octane index, represents a valid alternative to fossil fuels in internal combustion engines, especially in gasoline ones, and therefore the interest in ethanol for diesel engines is also increasing [7,8].

Ethanol is released into the atmosphere during its production, processing, transportation and use. For example, in the case of ethanol production by fermentation processes, considerable amounts of CO_2 and ethanol vapors are released, with losses up to 1.43 % of ethanol produced [9]. In the case of vehicles whose fuel includes ethanol, this organic compound can evaporate during refueling, operation and also when these vehicles are parked [10,11,12].In fact, the fuel tank, both at rest and in operation, is subjected to continuous evaporation, resulting in the release into the atmosphere of the most volatile components of gasoline [13,14,15], which therefore can be present in low concentrations in these environments. Although ethanol is not considered an extremely harmful pollutant, at high concentrations (above 1000 ppm) it can cause severe health problems, such as eye, skin and respiratory tract irritation, together with negative environmental effects [16]. Additionally, the mixture between high concentration ethanol and air can be explosive [17]. Considering this, and the increase in ethanol production, it is important to control its emissions and recovery with the object of improving technical and economic processes [10,11,18,19], with the consequent

increase in performance, both during the process of obtaining it [18,19], or during its use in vehicles.

Different technologies can be applied to control ethanol emissions, such as thermal oxidation, catalytic oxidation, biofiltration, absorption, adsorption, condensation and membrane separation [20]. Among them, adsorption has widely been accepted due to its effectiveness, easy operation and low cost [21], even at low concentration [22].

Adsorption takes place in porous solid, such as zeolites [23], mesoporous silica [24], porous clay [25] or in activated carbons (ACs) [26,27,28]. ACs with different morphologies are the most often used materials for this purpose due to their high specific surface areas and interesting textural properties [26-28]. As an example, activated carbons in form of pellets [29], granular activated carbons [30], powdered activated carbons [31,32], nanotubes [33], nanofibres [34], carbon monoliths [35] and, furthermore, spherical activated carbons (SACs) [36] can be used for organic compounds adsorption.

Spherical activated carbons (SACs) have acquired great interest in the recent years because of their advantages with respect to granular or powdered activated carbon, such as high wear resistance, high mechanical strength, good adsorption performance, high purity, low ash content, smooth surface, good fluidity, good packaging, low pressure drop, high micropore volume and more controllable pore size distribution [37,38]. Therefore, the development of the adsorbent properties of these materials is aim of continuous investigation.

In this sense, this study has been focused on activated carbons because they are well-used by the industry since they can be obtained from cheap and abundant precursors and by methodologies that are well-developed in industry and they are easily regenerable due to higher thermal stability.

Due to the polar nature of ethanol, it is also convenient to study the effect of the modification and/or development of surface oxygen groups in the SACs on the adsorption of ethanol. In fact, it has been found that the presence of ethanol (as gasoline additive) can modify in a positive or negative way the retention capacity of a canister to other hydrocarbons because of its polarity and its hygroscopic character [13,14]. In this regard, the concentration and nature of the surface oxygen groups in an AC can be modified by using different methods of oxidation [39,40] and/or heat treatments at different temperatures [41,42,43]. The oxidation treatments can be performed in liquid phase; for example using HNO_3 [44], H_2O_2 [44] or ammonium persulfate [44], or in gas phase, with carbon dioxide [45,46], steam [47] or air [48], although other treatments at room temperature such as oxygen plasma have also been used [49]. Because of oxidation, functional groups of different nature are formed. Also, thermal treatments in inert atmosphere at different temperatures can be used to modify the content of these oxygenated groups [42]. The characterization of these groups can be performed, among other techniques [50,51], by temperature programmed desorption (TPD) [41-43] as it causes decomposition of these groups as H_2O, CO_2 and CO. TPD coupled to some system for the evolved gas analysis (e.g. a mass spectrometer) permits the quantification of these groups from the integration of the desorption profiles of H_2O, CO_2 and CO [52].

5

The effect that oxygen surface groups have on the adsorption of polar adsorptives (especially water) has been deeply studied. However, few studies have analyzed its effect on phenol adsorption [53,54] and there are almost no data on SACs. Therefore, the aim of this work is to study the adsorption of ethanol on several types of SACs, paying special attention to the effect that the oxygen surface groups has on the ethanol adsorption, as a function of its relative pressure. Thus, our study focuses both on the low relative pressures range and on relative pressures close to unity. For this purpose, the results will be analyzed in three scenarios; i) ethanol concentration of 225 ppm, to cover the scarce existing data at this low concentration, as well as for security reasons, ii) ethanol adsorption at 1000 ppm, according to environmental regulations and health concerns that limit indoor concentrations [55] and iii) at high concentrations (ethanol relative pressure, near the unity), useful for other applications (e.g., canisters to retain high ethanol concentrations).

2. Experimental.

2.1. Materials.

In this work, a SAC supplied by Kureha Corporation (refered to as BAC) has been used as the main starting material [36]. A SAC derived from it, which was obtained through CO_2 activation [36] at 880 ℃ during 24 h (BAC58C) has also been used. In addition, other activated carbons, prepared from four different precursors, have been employed: two spherical activated carbons obtained from hydrothermal treatment of glucose and saccharose and subsequently activated with NaOH and CO_2 (samples GLUHT/N/3.0 and SACHT81C, respectively [56]); a granular activated carbon obtained from coconut fiber which has been activated with H_3PO_4 (CFMHI/70/4.1/3 [57]) and, finally, a

6

commercial granular activated carbon from Mead Westvaco (WVA1100, 10x25). Additionally, treated samples derived from them (by oxidation and/or heat-treatment) have been used. Information about these materials is summarized in Table 1, from the point of view of precursor, synthesis method, activating agent and post-treatment carried out.

Table 1. Some features of samples used in ethanol adsorption experiments

Sample	Precursor	Synthesis method	Activating agent	Post-treatment
BAC	Commercial	--		
BACA4	BAC	--	--	Oxidation with HNO_3
BACA4/900	BAC	--	--	Treatment at 900 ºC in N_2
BACOx400	BAC	--	--	Oxidation in air at 400 ºC
BACOx400/900	BAC	--	--	Treatment at 900 ºC in N_2
BAC58C	BAC	--	CO_2	--
BAC58CA4	BAC	--	CO_2	Oxidation with HNO_3
SACHT81C	Saccharose	Hydrothermal synthesis	CO_2	--
SACHT81CA4	Saccharose	Hydrothermal synthesis	CO_2	Oxidation with HNO_3
GLUHT/N/3.0	Glucose	Hydrothermal synthesis	NaOH	--
GLUHT/N/3.0/900	Glucose	Hydrothermal synthesis	NaOH	Treatment at 900 ºC in N_2
WVA1100	Wood	--	H_3PO_4	--
WVA1100/900	Wood	--	H_3PO_4	Treatment at 900 ºC in N_2
CFMHI/70/4.1/3	Coconut fiber	Impregnation	H_3PO_4	--

8

2.2. Oxidation process.

BAC was oxidized with 4 M HNO_3 solution, mixing 20 ml of the solution with 1 g of BAC for 2 h and, afterwards, the sample was washed with distilled water until neutral pH. In the case of air oxidation, BAC sample was air treated up to 400 ºC during 2 h in a horizontal quartz reactor (2 m long and 0.07 m diameter with a flow of 100 ml/min).

2.3. Thermal treatment.

The different materials oxidized both in air, or liquid phase, were thermally treated in nitrogen inert atmosphere to modify their oxygen contents (10 ºC/min up to 900 ºC) in the same horizontal quartz reactor (200 ml/min of N_2 flow and 2 h holding time at the maximum temperature, 900ºC).

Nomenclature of the materials (see Table 1) includes the name of the precursor (BAC) followed by the oxidation agent HNO_3 (N) or air (Ox) and, finally, in the case of the oxidation with HNO_3, the concentration of the HNO_3 solution (4 M), and in the case of the oxidation with air, the temperature (400 ºC). Also, the temperature of a post-treatment in N_2 (900 ºC) is included if this treatment is performed.

2.4. Textural characterization.

Textural characterization of all the samples was performed using N_2 adsorption at -196 ºC and CO_2 at 0 ºC [58] in a volumetric Autosorb-6B apparatus from Quantachrome. Before analysis, the samples were outgassed at 250 ºC for 4 h. The BET equation was applied to the nitrogen adsorption data to get the apparent BET surface area (S_{BET}). The Dubinin–Radushkevich equation was applied to the nitrogen adsorption data to determine the total micropore volume (pores with size < 2 nm) and to the carbon

9

dioxide adsorption isotherms to determine narrow micropore volumes (pores with size < 0.7 nm) [59]. The volume of mesopores (2 nm to 20 nm, Vmeso) was estimated as the difference between the volume (expressed as liquid) of N_2 adsorbed at $P\, Po^{-1} = 0.9$ and that adsorbed at $P\, Po^{-1} = 0.2$ [57].

2.5. Oxygen surface characterization.

Temperature-programmed desorption experiments were done in a DSC-TGA equipment (TA, SDT 2960 Simultaneous) coupled to a mass spectrometer (Balzers, OmniStar) to characterize the oxygen surface chemistry of all the samples [41,42]. In these experiments, 10 mg of sample were heated up to 950 ºC (heating rate 20 ºC/min) under a helium flow rate of 100 ml/min.

2.6. Ethanol adsorption.

Ethanol adsorption isotherms in all samples were obtained using an ASAP 2020 from Micromeritics. Before these tests, samples were outgassed for 4 hours under vacuum at 250ºC. From these adsorption isotherms, three relative pressure ranges were analysed, 0.003, 0.01 and 0.95, considering that ethanol saturation pressure at 25ºC is 58.75 mmHg [60]. These relative pressures would correspond to the following concentrations if the ethanol adsorption tests would be performed in flow at a total pressure of 760 mmHg and the other components in the stream would not be adsorbed: 225 ppm (P/Po = 0.003), 1000 ppm (P/Po = 0.01), and around 73000 ppm (P/Po = 0.95).

3. Results and discussion.

Adsorption processes on ACs usually depend both on porosity and surface chemistry of the absorbents [26-28]. Considering the polar character of ethanol, surface chemistry

10

might play an important role. For a better understanding of its importance, the effect of surface oxygen chemistry has to be separated from that of porosity. Thus, the ethanol adsorption results are firstly analyzed in five selected samples having different oxygen surface chemistry and very similar porosities. Secondly, the results obtained with nine additional samples, which differ in porosity and surface chemistry are studied, have been analysed to study both the effect of porosity and surface chemistry.

3.1. Porosity of BAC samples.

Figure 1 presents the N_2 adsorption isotherms (at -196 °C) of the spherical activated carbon BAC, the samples oxidized with air (BACOx400), HNO_3 (BACA4), and those samples thermally treated (BACA4/900 and BACOx400/900).
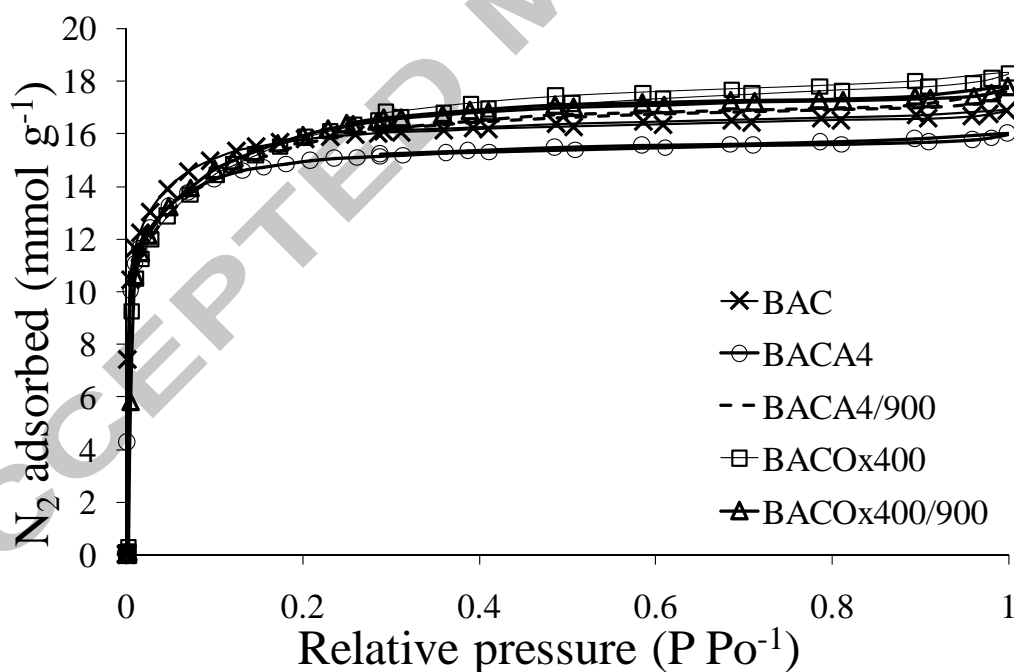

Figure 1. N_2 adsorption-desorption at -196 °C of BAC, samples oxidized with air (BACOx400), HNO_3 (BACA4), and thermally treated samples (BACA4/900 and BACOx400/900).

11

From Figure 1 it can be observed that: i) the SACs are microporous adsorbents (isotherms type I), ii) these samples have high and quite similar adsorption capacities, iii) the treatments performed, both oxidation and thermal treatment in inert atmosphere, do not significantly change the shape of the adsorption isotherms, especially for relative pressures lower than 0.2, in relation to the original BAC precursor. Table 2 shows the textural properties of these SACs deduced from N_2 and CO_2 adsorption isotherms.

Table 2. Textural properties of the SACs.

Sample	S_{BET} $(m^2\,g^{-1})$	$V_{DR}N_2$ $(cm^3\,g^{-1})$	$V_{DR}CO_2$ $(cm^3\,g^{-1})$
BAC	1291	0.55	0.44
BACA4	1212	0.53	0.46
BACA4/900	1190	0.54	0.40
BACOx400	1152	0.54	0.43
BACOx400/900	1189	0.55	0.40

Table 2 shows that, in agreement with the observations extracted from the adsorption isotherms, all these SACs have similar adsorption capacities. Consequently, surface areas of the SACs are very similar (between 1150 and 1300 $m^2\,g^{-1}$), as well as their total micropore volumes ($V_{DR}N_2$ between 0.53 and 0.55 $cm^3\,g^{-1}$) and their narrow micropore volumes ($V_{DR}CO_2$ between 0.40 and 0.46 $cm^3\,g^{-1}$).

Interestingly, these SACs present similar textural properties, and hence the effect that their different surface oxygen contents might have on ethanol adsorption can be well analyzed.

3.2. Oxygen surface chemistry in BACs samples.

In general, surface oxygen chemistry influences the adsorption of VOCs [26,27]. If the VOC is polar, the effect of the oxygenated groups can be more important, being influenced by the polarity of the compound. Water is one of the most studied polar adsorptives given the industrial use of the activated carbons [61,62]. Many of the published results regarding water adsorption on activated carbons show that surface oxygen groups have more influence on the adsorption at low relative pressures [61,62]. Since the polarity of ethanol is lower than that of water (the dipole moments of ethanol and water are 1.69 D and 1.85 D, respectively [63]), the effect of oxygen groups on the adsorption of ethanol should be expected to be likely less important. The lack of data and the current increasing interest of ethanol recommend further research.

Figure 2 (a and b), obtained from the TPD runs, shows CO_2 and CO desorption profiles for all the BAC samples and their integration allows to quantify oxygen groups that decompose as H_2O, CO_2 or CO. Table 3 summarizes the results obtained and the total oxygen contents deduced from them ($O_T = H_2O + 2CO_2 + CO$).

Both from Figure 2 and Table 3 it can be observed that the type of oxidant used (air or HNO_3) significantly affects both their oxygen contents, and their oxygen functionalities. Thus, air oxidation of the BAC sample produces higher oxygen contents than HNO_3 (compare in Table 3, the total oxygen contents of samples oxidized with air, 7076 μmol g^{-1}, and with HNO_3, 3312 μmol g^{-1}). However, HNO_3 generates more CO_2 at temperatures below 500 °C than air. All these results agree with previous observations showing that the generation of surface oxygen groups largely depends on the nature of

13

the oxidizing agent used [39-40]. Finally, Figure 2 and Table 3 show that the thermal treatment reduces, as expected, the surface oxygen groups in the SACs.
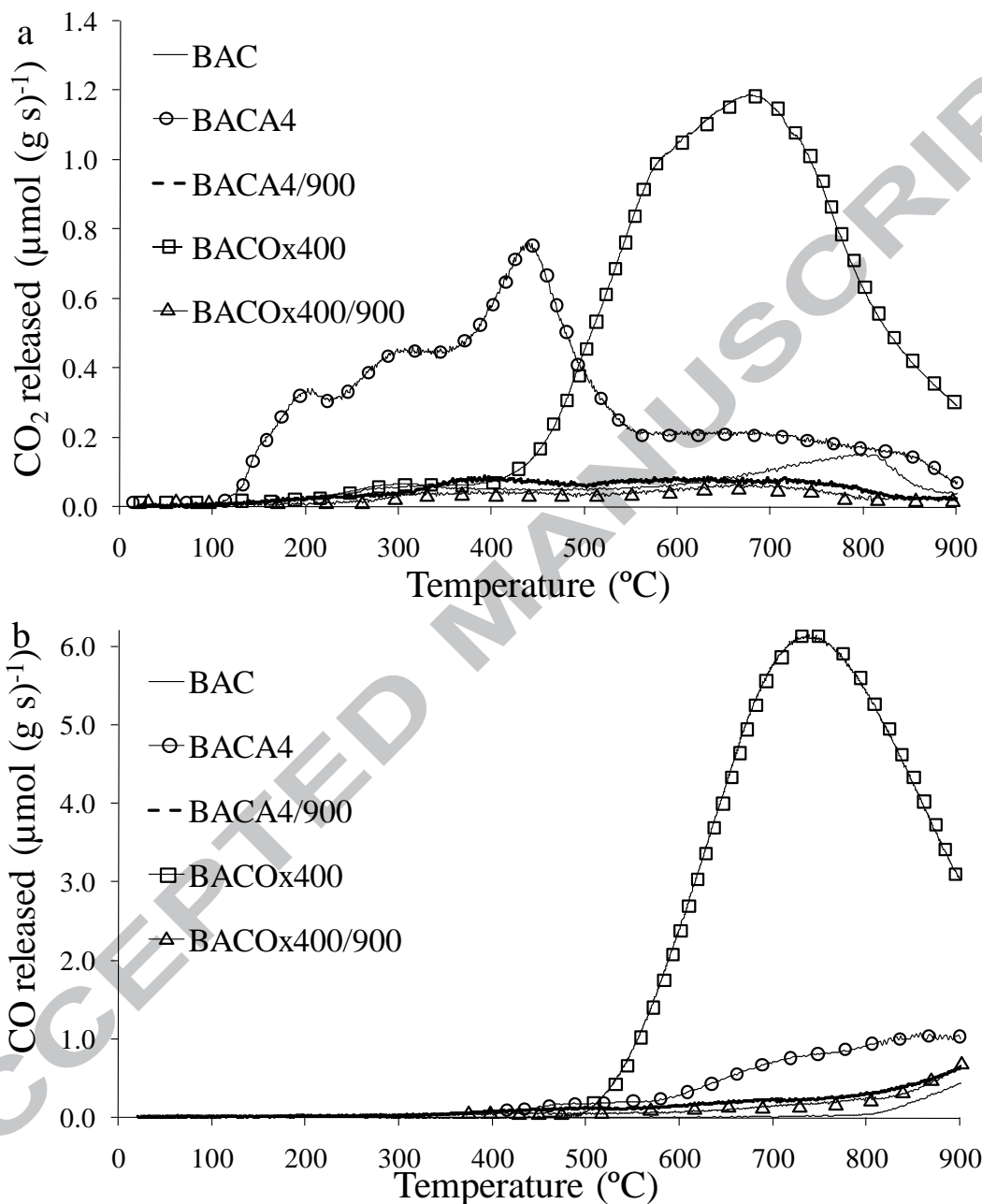

Figure 2. Desorption profiles of CO_2 (a) and CO (b) for BAC and its oxidized and thermally treated derived samples.

14

Table 3. Quantification of the oxygen groups that decompose as H_2O, CO_2 or CO and total oxygen content.

Sample	H_2O μmol/g	CO_2 μmol/g	CO μmol/g	O_T^1 μmol/g	CO_2 (μmol/g)			CO (μmol/g)		
					Carboxyl	Anhydrides	Lactones	Anhydrides	Phenols	Carbonyls[2]
BAC	455	167	231	1020	58	29	81	0	0	231
BACA4	573	663	1413	3312	175	182	167	215	657	483
BACA4/900	30	134	467	764	27	68	12	99	82	286
BACOx400	250	1095	4636	7076	31	202	862	199	1962	2475
BACOx400/900	18	82	272	454	6	27	45	29	106	137

[1] Total oxygen content $O_T = H_2O + 2CO_2 + CO$

[2] Carbonyl groups included quinones and ethers.

15

3.3. Ethanol adsorption.

Figure 3 shows the ethanol adsorption isotherms at 25 ℃ on BAC and on the oxidized and thermally treated samples derived from it. These isotherms will be first analysed up to relative pressures close to unity.

3.3.1. Ethanol adsorption isotherms at relative pressures close to unity.

The comparison between N_2 adsorption isotherms (Figure 1) and ethanol adsorption isotherms (Figure 3) shows that the shapes of these isotherms are similar, despite the fact that the shapes of the adsorption isotherms are affected by the experimental conditions, (e.g., saturation pressure of the adsorptive, 58.75 mmHg for ethanol at 25 ℃ and 760 mmHg for N2 at -196 ℃).
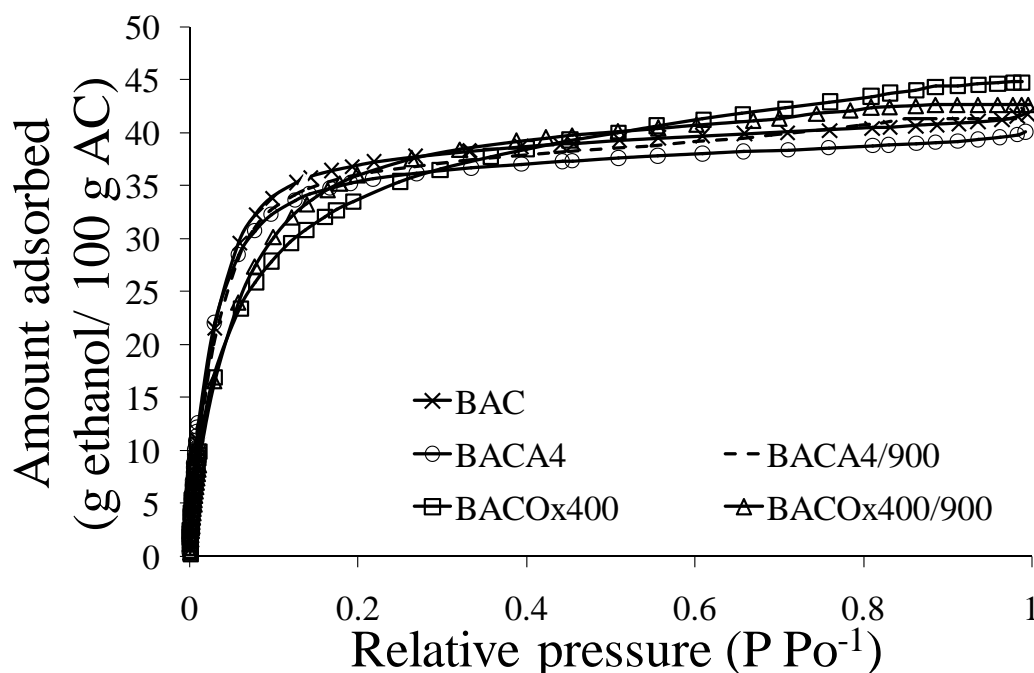

Figure 3. Ethanol adsorption isotherms at 25 ℃ for BAC, and the oxidized and thermally treated samples derived from it.

The SACs studied show very similar ethanol adsorption capacities, especially at high relative pressure, suggesting that oxidation treatments and subsequent thermal

treatments in inert atmosphere do not appreciably affect the ethanol adsorption capacity. These results are in agreement with the fact that adsorption of any adsorptive, at relative pressure close to unity, mainly depends on the porosity of the material. This well-known and accepted observation is clearly supported by many examples where the Gurvitsch rule was applied or commented [35,64,65].

In this sense, since the five SACs studied have similar porosities, their adsorption capacities of nitrogen and ethanol, expressed as liquids, are comparable at relative pressures close to unity, as it can be seen in Table 4. It can be confirmed that, for a relative pressure of 0.95, the ratios of the volume of ethanol adsorbed and the volume of nitrogen absorbed (expressed both as liquids) are very close to unity for the five samples (in the range of 0.89 to 0.92).

Table 4. Comparison of Gurvitsch rule in the SACs studied (the adsorbed volumes were calculated at $P/Po=0.95$)

Sample	$V_{ads}N_2$ $(cm^3 \, g^{-1})$	$V_{ads}Ethanol$ $(cm^3 \, g^{-1})$	$V_{ads}Ethanol \, / \, V_{ads}N_2$
BAC	0.58	0.51	0.89
BACA4	0.55	0.49	0.89
BACA4/900	0.59	0.53	0.90
BACOx400	0.62	0.55	0.89
BACOx400/900	0.60	0.53	0.92

These observations indicate that the amount of ethanol adsorbed, especially at relative pressures close to unity, depends only on the porosity of the samples and not on their surface oxygenated groups content. This fact suggests, at first sight, that the polarity of ethanol and its interaction with oxygen groups are not important at these experimental conditions.

17

A more detailed analysis of Figure 3 at low relative pressures allows advancing that oxygenated groups appear to have some influence on ethanol adsorption. In fact, it can be observed that the isotherms at low relative pressures cross at relative pressures greater than 0.2. For this reason, next we analyse the ethanol adsorption isotherms at low relative pressures.

3.3.2. Ethanol adsorption isotherms at low relative pressures.

Figure 4 presents the magnification of the ethanol adsorption isotherms at low relative pressures using a logarithmic scale from 0.001 to 0.01. Two relative pressure zones have been selected; 0.003 (225 ppmv concentration) and 0.01 (1000 ppmv concentration). Figure 4 shows that, in general, the isotherms are parallel at low relative pressures (<0.003), although two samples cross each other at relative pressure of 0.001, and this trend changes as the relative pressure range increases. Thus, up to 0.01 the adsorption capacities of the samples vary. Additionally, Table 4 allows observing that about 10 % of the narrow micropore volume of each sample is not occupied (i.e., the ethanol adsorbed does not totally filling the available narrow microporosity). These observations suggest that ethanol adsorption at low concentration could be influenced by differents factor such as the oxygen contents and oxygen functionalities, the external surface area, the pore size distribution of the wider pores, the different adsorption temperatures and the different molecular diameters of ethanol (0.45 nm) and nitrogen (0.30 nm). Thus, ethanol might be adsorbed up to a lower extent than nitrogen.
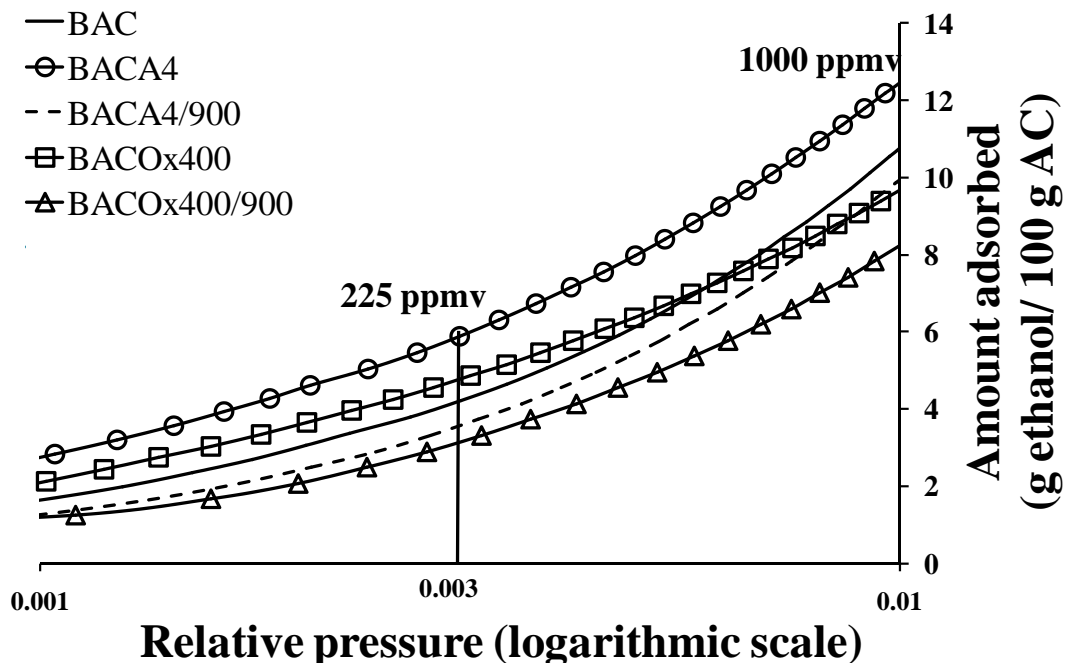
18

Figure 4. Ethanol adsorption isotherms at low relative pressures.

In this sense, from Figure 4 and Table 3 it can be concluded that for relative pressures lower than 0.01 (concentrations lower than 1000 ppmv), ethanol adsorption is influenced by the surface oxygenated groups content. The SACs presenting the highest ethanol adsorption are those that have been oxidized, the samples thermally treated in inert atmosphere present the lowest ethanol adsorption and the original BAC precursor has an intermediate adsorption capacity. At low pressures, ethanol adsorption depends on the samples oxygen content, although not linearly; the ethanol adsorption capacity of the original BAC sample (O_T = 1020 µmol g^{-1}) is 4.22 g ethanol/100 g AC, for the sample oxidized with air (O_T = 7076 µmol g^{-1}) is 4.55 g ethanol/100 g AC and for the sample oxidized with 4M HNO_3 solution (O_T = 3312 µmol g^{-1}) is 5.45 g ethanol/100 g AC. Samples thermally treated, that have lower oxygen contents, also present lower ethanol adsorption capacities; ethanol adsorption capacity for BACA4/900 (O_T = 764 µmol g^{-1}) is 3.37 g ethanol/100 g AC, and for sample BACOx400/900 (O_T = 454 µmol g^{-1}) is 2.89 g ethanol/100 g AC.

19

These results confirm that at these low relative pressures, the oxygenated groups have a significant influence on the ethanol adsorption capacity. However, the fact that the sample with highest ethanol adsorption capacity (BACA4) is not the sample with highest oxygenated groups content confirms that also the nature of the oxygen groups seems to affect the interaction between the adsorbent and ethanol.

Using the methodology published elsewhere [52], deconvolution of the TPD profiles (H_2O, CO_2 and CO) have been performed to get information and to estimate the content of the different surface oxygenated functionalities. Anyway, it is important to recall that the values obtained from these deconvolution curves should only be considered as estimated values due to possible secondary reactions, such as the reaction of Boudard [66]. In this reaction (*CO_2 +C ↔ 2CO + Energy (122 kJ/mol)*), the formation of CO from CO_2 or, conversely, the generation of CO_2 from CO, occur simultaneously and, hence, the formation of CO or CO_2 cannot be quantified independently.

The evolution of these three compounds can be explained as follow: i) H_2O, besides being mostly adsorbed on the samples, could also arise from internal changes in carboxyl to anhydrides groups, ii) CO_2 is derived from carboxyl groups and derived compounds (anhydrides and lactones) and iii) CO comes from the carbonyl, phenolic and ether groups. In general, the accepted temperature decomposition ranges for groups evolving as CO_2 are: between 150 and 350 °C for the carboxylic acids [67], between 350 and 400° C for anhydrides [67] (that also give CO), and between 350 and 650 °C for lactones and lactols [68]. The temperatures of groups that evolve as CO are: between 350 and 400 ° C for anhydrides [67] (which also give CO_2), between 600 and 700 °C for phenols [67], and between 700 and 1000 ° C for carbonyls, quinones and ethers [67].

20

As an example, Figure 5 shows the deconvolution of the profiles of CO_2 and CO in BACOx400/900 sample and the assignation made to obtain individual peaks, corresponding to the functional oxygen groups and Table 3 summarizes the results obtained. These results confirm the following general aspects: 1) the precursor BAC has a low content of surface oxygenated groups, 2) after oxidation (independently of the oxidizing agent used) there is an increase in the oxygen groups content, 3) air oxidation is more selective to the creation of phenols and carbonyls, whereas oxidation with HNO_3 is more selective to the creation of carboxyl groups, 4) the samples thermally treated in an inert atmosphere have significantly reduced their oxygen groups and 5) anhydride contents obtained by deconvolution from CO_2 and CO profiles are quite similar, which indicates the reliability of the analysis.
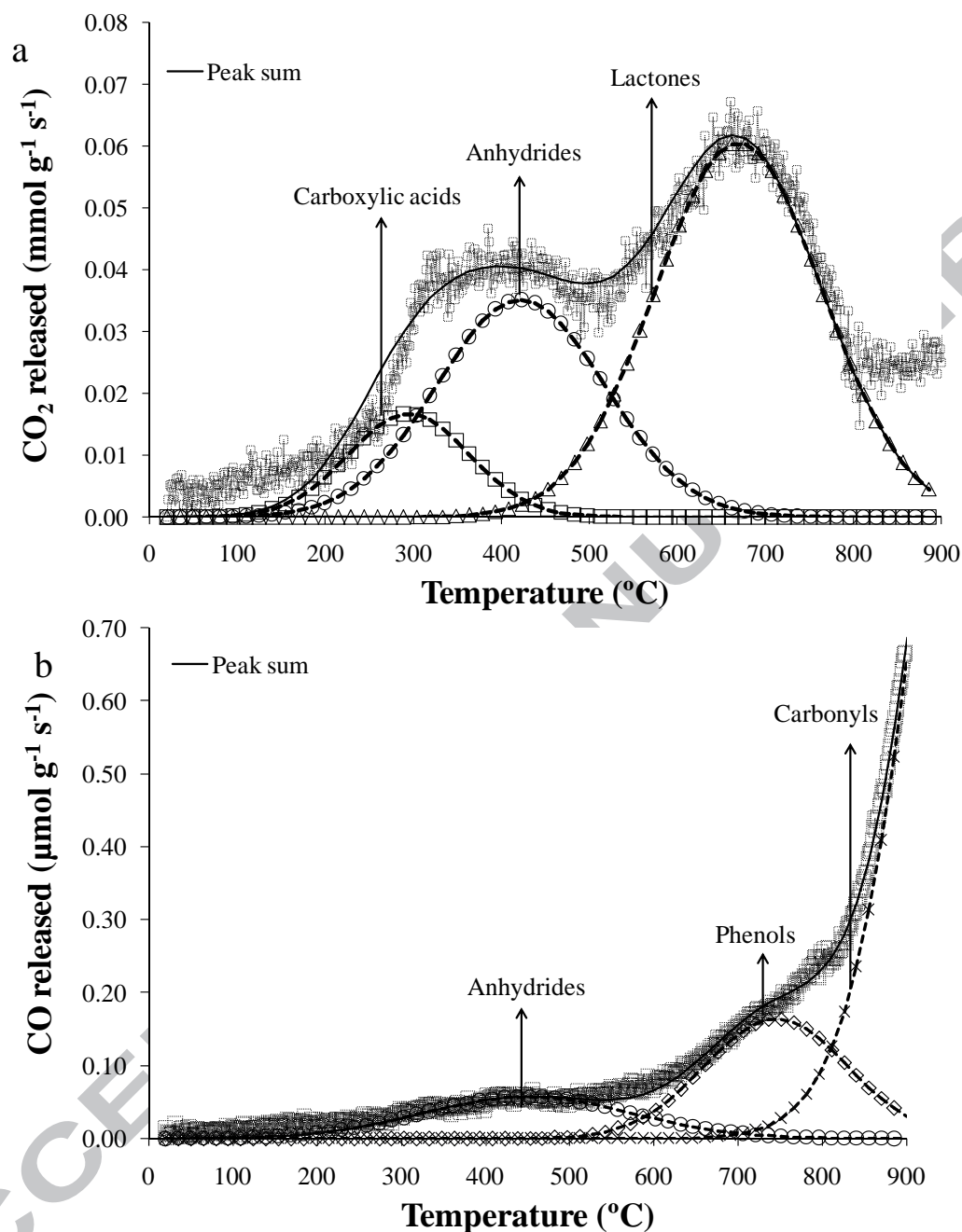
Figure 5. Deconvolution of the profiles of CO_2 (a) and CO (b) in BACOx400/900 sample.

Regarding ethanol adsorption and the deconvolution results it can be concluded: i) that ethanol adsorption at a concentration of 225 ppmv is favoured by the carboxyl and anhydride groups, ii) the presence of phenolic, carbonyl groups and their derivatives does not benefit the ethanol-adsorbent interactions and iii) for higher ethanol

22

concentrations, when the ethanol adsorption isotherms cross, the importance of the carboxyl and anhydride groups in the adsorption of ethanol decrease, being porosity the key factor controlling ethanol adsorption.

To confirm that this result is not limited to SACs, ethanol adsorption has been extended to activated carbon samples having different morphologies, porosities and oxygenated groups contents.

3.3.3. Ethanol adsorption on activated carbons of different nature and porosity.

Figure 6 shows the N_2 adsorption isotherms at -196 °C of the new samples and Table 5 compiles their textural characterization (see nomenclature in Table 1). From this figure it can be deduced, in agreement with the shape of the isotherms, that the activated carbons have different porosity distributions: some are activated carbons with type I isotherm, characteristic of microporous carbons, and others are activated carbons with type IV isotherm (e.g. CFMHI/70/4.1/3 sample), characteristic of mesoporous carbons.
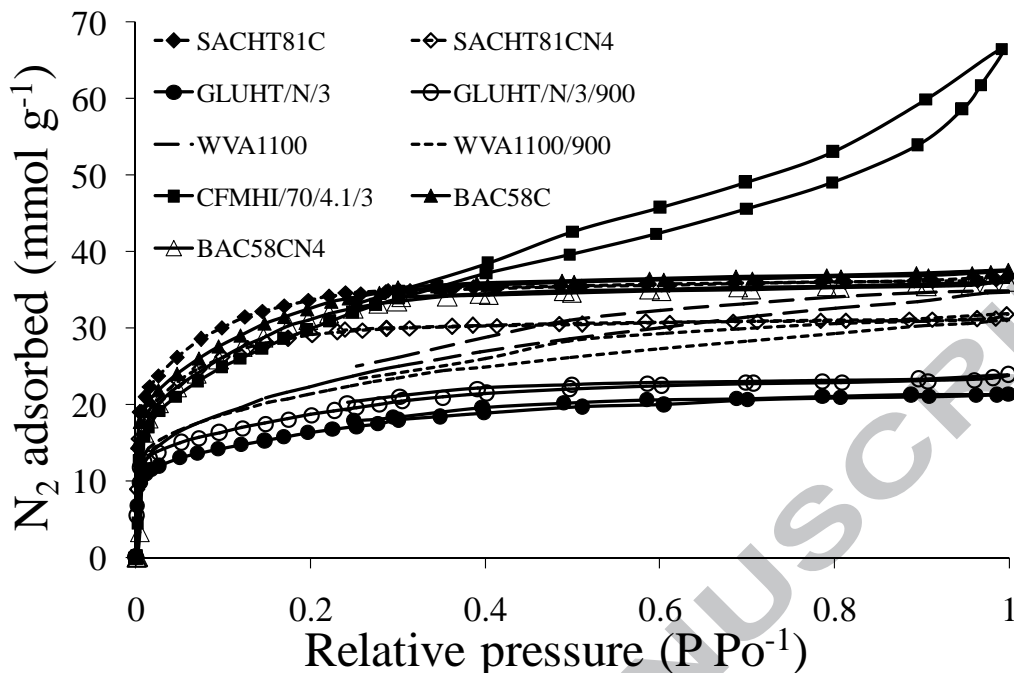
Figure 6. N_2 adsorption-desorption at -196 °C for the samples from different nature.

Table 5. Textural properties of the activated carbons from different nature.

Sample	S_{BET} $(m^2 g^{-1})$	$V_{DR}N_2$ $(cm^3 g^{-1})$	$V_{DR}CO_2$ $(cm^3 g^{-1})$	V_{meso} $(cm^3 g^{-1})$
BAC58C	2586	1.05	0.56	0.15
BAC58CA4	2410	0.98	0.54	0.15
SACHT81C	2555	1.15	0.69	0.09
SACHT81CA4	2252	1.00	0.58	0.07
GLUHT/N/3.0	1270	0.54	0.37	0.15
GLUHT/N/3.0/900	1452	0.61	0.41	0.16
WVA1100	1757	0.67	0.36	0.70
WVA1100/900	1457	0.59	0.31	0.70
CFMHI/70/4.1/3	2438	0.97	0.49	0.84

Table 5 shows that the activated carbons have different porosity developments,

according to the shape of the adsorption isotherms. The values of the surface areas are

between 1270 and 2586 $m^2 g^{-1}$, the micropore volumes are between 0.54 and 1.15 $cm^3 g^1$

and the narrow micropore volumes are between 0.31 and 0.69 $cm^3 g^{-1}$. The hysteresis

cycles and the large contribution of mesopores in samples WVA1100 and

CFMHI/70/4.1/3 must be highlighted, being the mesopore volumes for these samples 0.70 and 0.84 cm^3 g^{-1}, respectively.

Figure 7 shows ethanol adsorption isotherms for these samples. Again, the similarity between nitrogen adsorption isotherms (Figure 6) and ethanol isotherms (Figure 7) must be remarked, despite the different adsorption temperatures used. Therefore, as previously mentioned, when relative pressure increases the microporosity of the samples is progressively filled, which explains that porosity is the most important parameter influencing ethanol adsorption. Thus, at relative pressures close to unity, the microporosity is filled with any of the two adsorbates, nitrogen or ethanol.
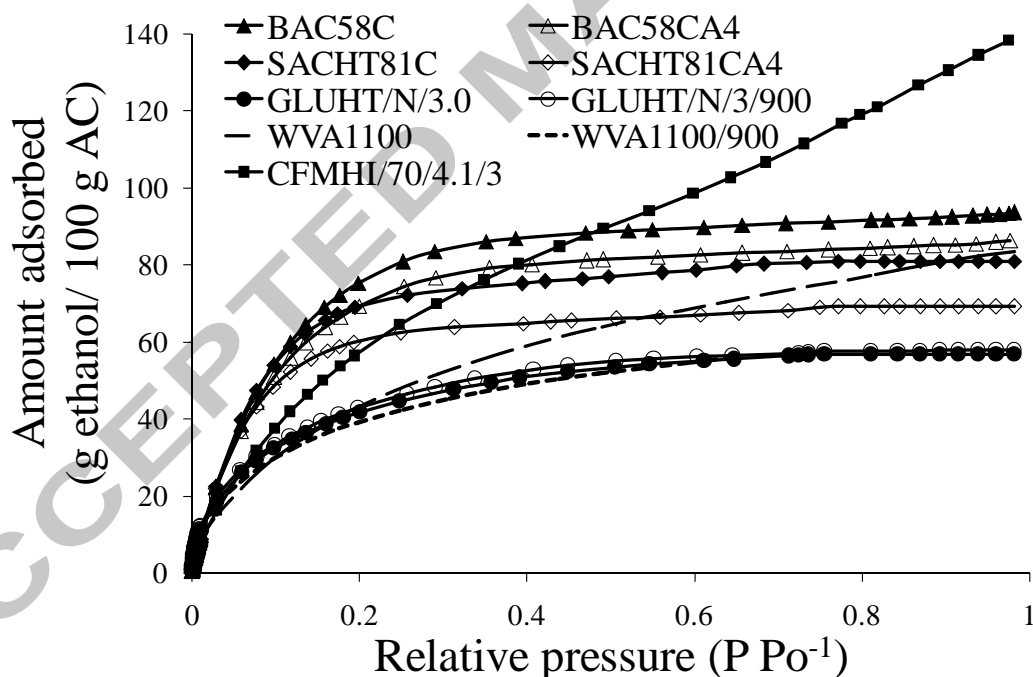

Figure 7. Ethanol adsorption isotherms at 25 ºC for the samples from different nature.

From comparison between Figures 6 and 7 it can be stated that CFMHI/70/4.1/3 sample, which has the highest nitrogen adsorption capacity (see Figure 6), largely due to its high

25

volumes of micro and mesopores, also presents the highest ethanol adsorption capacity (see Figure 7).

The above comments (section 3.3.1) regarding the effect of surface chemistry, are furthermore confirmed, observing the adsorption isotherms of all the samples at relative pressure close to unity. For example, when comparing the isotherms of samples BAC58C and SACHT81C with those of their samples oxidized with HNO_3 (BAC58CA4 and SACHT81CA4, respectively). If the oxygenated surface groups were important in this relative pressure range, the ethanol adsorption capacity should be greater for the oxidized samples BAC58CA4 (86 g ethanol/100 g AC) and SACHT81CA4 (69 g ethanol/100 g AC) than for BAC58C (94 g ethanol/100 g AC) and SACHT81C (81 g ethanol/100 g AC), contrarily to what is observed in Figure 7. The decrease in textural properties (i.e. surface area and micropore volumes) after oxidation explains the lower ethanol adsorption capacities of the oxidized samples in comparison to the original ones (see Table 5).

All these results have shown that ethanol adsorption at relative pressures close to unity is mainly governed by the porosity and not by the oxidation or thermal treatments performed over the samples. These observations are clearly confirmed in Figure 8, which presents the ethanol adsorption capacities versus nitrogen adsorption ones (expressed as liquids) at relative pressure of 0.95. From this figure it is confirmed that Gurvitsch rule explains the behavior of the 14 samples studied (including the five samples studied in the first part, at low relative pressures), although their surface oxygenated groups contents are significantly different. The good correlation between the amount of nitrogen and ethanol adsorbed from Figure 8 allows to conclude that

26

ethanol adsorption at relative pressure close to unity is mainly governed by the porosity

of the samples, regardless the contents in oxygenated groups resulting from the different
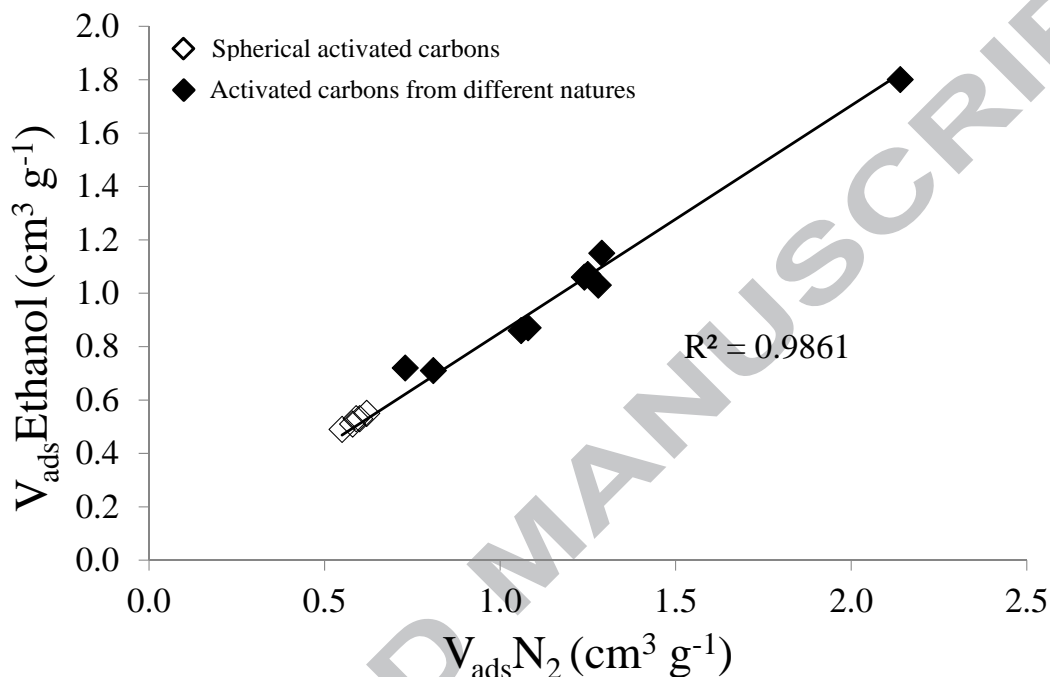
treatments.

Figure 8. Relation between volumes of N_2 and ethanol adsorbed (as liquids) at relative pressure close to unity ($P/Po = 0.95$). Filled markers correspond to samples studied in this section and empty markers to the samples studied in the first section.

4. CONCLUSIONS

In the present paper the adsorption of ethanol on activated carbons with different

morphologies and oxygen surface chemistry have been studied focusing on three

relative pressure ranges. The results at low ethanol relative pressures adsorption on five

spherical activated carbons which have similar textural properties but different oxygen

surface chemistry show that surface chemistry has an important influence on the ethanol

adsorption capacity. This influence is not due to the total oxygen content of the sample,

but especially to the kind/nature of these oxygen functional groups that influence

27

ethanol adsorption capacity at low concentration. Thus, the presence of carboxyl and anhydride groups favours ethanol adsorption at low concentration, whereas the presence of phenols and carbonyls is negative. Among the oxidation treatments studied, the oxidation with 4M HNO_3 shows the best performance in these conditions.

On the contrary, the analysis performed at high ethanol concentration shows that the adsorption capacities depend only on the porosity, and not on the surface chemistry of the ACs, which is confirmed by the 14 samples selected and studied. In particular, the total micropore volume governs ethanol adsorption in these conditions.

5. ACKNOWLEDGMENTS

6. REFERENCES

[1]   Vilar RB, Da Silva R, Schossler P, Cataluña Veses R, Piatnicki CMS, Samios D, Caramão EB. Preliminary characterization of anhydrous ethanol used in Brazil as automotive fuel. Journal of Chromatography A 2003;985:367-73.

[2]   Jørgensen H, Kristensen JB, Felby C. Enzymatic conversion of lignocellulose into fermentable sugars: challenges and opportunities. Biofuels, Bioprod. Bioref. 2007;1:119-34.

[3]   Chin JY, Batterman SA. VOC composition of current motor vehicle fuels and vapors, and collinearity analyses for receptor modeling. Chemosphere 2012;86:951-58.

[4]   Anderson JE, DiCicco DM, Ginder JM, Kramer U, Leone TG, Raney-Pablo HE, Wallington TJ. High octane number ethanol-gasoline blends: Quantifying the potential benefits in the United States. Fuel 2012;97:585-94.

[5]   Balat M. Global bio-fuel processing and production trends. Energy Explor Exploit 2007;25:195–218.

[6]   Renewables Energy Policy Network for the 21st Century (REN21). Renewable 2012 Global Status Report. Paris: REN21 Secretariat and Washington, DC: Worldwatch Institute; 2012.

[7]   Rakopoulos DC, Rakopoulos CD, Papagiannakis RG, Kyritsis DC. Combustion heat release analysis of ethanol or n-butanol diesel fuel blends in heavy-duty DI diesel engine Fuel 2011;90:1855-67.

[8]   Torres-Jimenez E, Svoljšak Jerman M, Gregorc A, Lisec I, Dorado MP, Kegl B. Physical and chemical properties of ethanol-diesel fuel blends. Fuel 2011;90:795-802.

[9]   Domenech-López F, Lorenzo-Acosta Y, Lorenzo-Izquierdo M, Esquivel-Baró L. Diagnóstico preliminar de las emisiones gaseosas en la industria de los derivados de la caña de azúcar. ICIDCA sobre los derivados de la caña de azúcar. 2011;45:30-37.

[10]   Viggiano A, Magi V. A comprehensive investigation on the emissions of ethanol HCCI engines. Applied Energy 2012;93:277-87.

[11]   Monteiro-Sales LC, Sodré JR. Cold start emissions of an ethanol-fuelled engine with heated intake air and fuel. Fuel 2012;95:122-5.

[12]   Martines-Filho J, Burnquist HL, Vian CEF. Bioenergy and the rise of sugarcane based ethanol in Brazil. Choices 2006;21:91-6.

[13]   Grisanti AA, Aulich TR, Knudson CL. Gasoline Evaporative Emissions: Ethanol Effects on Vapor Control Canister Sorbent Performance. SAE Technical Paper No. 952748.

[14]   Air Quality Impacts of the Use of Ethanol in California Reformulated Gasoline. Final Report to the California Environmental Policy Council. California Environmental Protection. Agency Air Resources Board. 1999.

[15]   European commission. Institute for Environment and Sustainability. Joint EUCAR/JRC/CONCAWE Study on: Effects of gasoline vapour pressure and ethanol content on evaporative emissions from modern cars. 2007

[16]   Anastas PT, Warner JC. Green chemistry. Theory and Practice, New York: Oxford University Press; 1998.

[17]   http://www.insht.es/InshtWeb/Contenidos/Documentacion/FichasTecnicas/ FISQ/Ficheros/0a100/nspn0044.pdf

[18]   Taylor F, Kurantz MJ, Goldberg N, Craig JC. Control of Packed Column Fouling in the Continuous Fermentation and Stripping of Ethanol. Biotechnology and Bioengineering 1996;51:33-9.

[19]   Eyng E, Vasconcelos da Silva F, Palú F, Frattini-Fileti AM. Neural Network Based Control of an Absorption Column in the Process of Bioethanol Production. Brazilian Archives of Biology and Technology 2009;52:961-72.

[20]   Khan FI, Ghoshal AK, Removal of volatile organic compounds from polluted air, J. Loss Prev. Process Ind. 2000;13:527–45.

[21]   Ruhl MJ, Recover VOCs via adsorption on activated carbon, Chem. Eng. Prog. 89 (1993) 37–41.

[22] Fletcher AJ, Yüzak Y, Thomas KM. Adsorption and desorption kinetics for hydrophilic and hydrophobic vapors on activated carbon. Carbon 2006;44:989-1004.

[23] Hu Q, Li JJ, Hao ZP, Li LD, Qiao SZ. Dynamic adsorption of volatile organic compounds on organofunctionalized SBA-15 materials. J Chem Eng 2009;149:281–8.

[24] Dou B, Hu Q, Li J, Qiao S, Hao Z. Adsorption performance of VOCs in ordered mesoporous silicas with different pore structures and surface chemistry. Journal of Hazardous Materials. 2011;186:1615-24.

[25] Qu F, Zhu L, Yang K. Adsorption behaviors of volatile organic compounds (VOCs) on porous clay heterostructures (PCH). Journal of Hazardous Materials. 2009;170:7-12.

[26] Lillo-Ródenas MA, Cazorla-Amorós D, Linares-Solano A. Behaviour of activated carbons with different pore size distributions and surface oxygen groups for benzene and toluene adsorption at low concentrations. Carbon 2005;43:1758–67.

[27] Lillo-Ródenas MA, Fletcher AJ, Thomas KM, Cazorla-Amorós D, Linares-Solano A. Competitive adsorption of a benzene–toluene mixture on activated carbons at low concentration. Carbon 2006;44:1455–63.

[28] Carratalá-Abril J, Lillo-Ródenas MA, Linares-Solano A, Cazorla-Amorós D. Activated carbons for the removal of low concentration gaseous toluene at the semipilot scale. Ind Eng Chem Res 2009;48:2066–75.

[29] Watanabe F, Kozuka J, Ito M, Hasatani M. Heat and Mass Transfer in Super Active Carbon/Ethanol Adsorption Heat Pump with a Packed Bed Type Adsorber. Heat Transfer-Japanese Research 1996;25:466-75.

[30]   Gales L, Mendes A, Costa C. Hysteresis in the cyclic adsorption of acetone, ethanol and ethyl acetate on activated carbon. Carbon 2000;38:1083-8.

[31]   Do DD, Do HD. Characterization of Micro-Mesoporous Carbonaceous Materials. Calculations of Adsorption Isotherm of Hydrocarbons. Langmuir 2002;18:93-9.

[32]   Bae JS, Do DD. On the equilibrium and dynamic behavior of alcohol vapors in activated carbon. Chemical Engineering Science 2006;61:6468-77.

[33]   Shih YH, Li MS. Adsorption of selected volatile organic vapors on multiwall carbon nanotubes. Journal of Hazardous Materials. 2008;154:21-8.

[34]   El-Sharkawy II, Saha BB, Koyama S, He J, Ng KC, Yap C. Experimental investigation on activated carbon–ethanol pair for solar powered adsorption cooling applications. International journal of refrigeration 2008;31:1407-13.

[35]   Fuertes AB, Marbán G, Nevskaia DM. Adsorption of volatile organic compounds by means of activated carbon fibre-based monoliths. Carbon 2003;41:87–96.

[36]   Romero-Anaya AJ, Lillo-Ródenas MA, Linares-Solano A. Spherical activated carbons for low concentration toluene adsorption. Carbon 2010;48:2625-33.

[37]   Liu Z, Ling L, Qiao W, Liu L. Effect of hydrogen on the mesopore development of pitchbased spherical activated carbon containing iron during activation by steam. Carbon 1999;37:2063–66.

[38]   Wang Q, Liang XY, Zhang R, Liu CJ, Liu XJ, Qiao WM, et al. Preparation of polystyrene-based activated carbon spheres and their adsorption of dibenzothiophene. New Carbon Materials 2009;24:55-60.

[39]   Molina-Sabio M, Muñecas-Vidal MA, Rodríguez-Reinoso F. Modification in Porous Texture and Oxygen surface groups of activated carbon by oxidation.

Studies in surface science and catalysis "Characterization of porous solids II". 1991;62:329-39.

[40] Moreno-Castilla C, López-Ramón MV. Carrasco-Marín F. Changes in surface chemistry of activated carbons by wet oxidation. Carbon 2000;38:1995-2001.

[41] Román-Martínez MC, Cazorla-Amorós D, Linares-Solano A, Salinas-Martínez de Lecea C. TPD and TPR characterization of carbonaceous supports and Pt/C catalysts. Carbon 1993;31:895-902.

[42] De Miguel SR, Román-Martínez MC, Jablonski EL, Fierro JLG, Cazorla-Amorós D, Scelza OA. Characterization of Bimetallic PtSn Catalysts Supported on Purified and H_2O_2- Functionalized Carbons Used for Hydrogenation Reactions. Journal of Catalysis 1999;184:514-25.

[43] Calo JM, Cazorla-Amorós D, Linares-Solano A, Román-Martínez MC, Salinas-Martínez de Lecea C. The effects of hydrogen on thermal desorption of oxygen surface complexes. Carbon 1997;35:543-54.

[44] Moreno-Castilla C, Ferro-García MA, Joly JP, Bautista-Toledo I, Carrasco-Marín F, Rivera-Utrilla J. Activated carbon surface modifications by nitric acid, hydrogen peroxide, and ammonium peroxydisulfate treatments. Langmuir 1995;11:4386-92.

[45] Teng H, Ho JA, Hsu YF, Hsieh CT. Preparation of Activated carbons from Bituminous Coals with CO_2 Activation. 1. Effects of oxygen content in raw coals. Industrial and Engineering Chemistry Research 1996;35:4043-49.

[46] Teng H, Hsieh CT. Influence of Surface Characteristics on Liquid-Phase Adsorption of Phenol by Activated Carbons Prepared from Bitominous Coal. Industrial and Engineering Chemistry Research 1998;37:3618-36.

33

[47]   Jia YA, Thomas KM. Adsorption of Cadmium on oxygen surface sites in activated carbon. Langmuir 2000;16:1114-22.

[48]   Gómez-Serrano V, Pastor-Villegas J, Durán-Valle CJ, Valenzuela-Calahorro C. Heat treatment of rockrose char in air. Effect on surface chemistry and porous texture. Carbon 1996;34:533-38.

[49]   Quirós M, García AB, Montes-Morán MA. Influence of the support surface properties on the protein loading and activity of lipase/mesoporous carbon biocatalysts. Carbon 2011;49:406-15.

[50]   Boehm HP. Surface Chemical Characterization of Carbons from Adsorption Studies. In: Bottani and Tascón editors. Adsorption by Carbons 2008, Pages 301-327.

[51]   Strelko V, Malik DJ, Streat M. Characterisation of the surface of oxidised carbon adsorbents. Carbon 2002;40:95–104.

[52]   Figueiredo JL, Pereira MFR, Freitas MMA, Orfao JJM. Modification of the surface chemistry of activated carbons. Carbon 1999;37:1379-89.

[53]   Liu CJ, Liang XY, Teng N, Liu XJ, Long DH, Zhan L, et al. The surface chemistry of pitch-based spherical activated carbon (PSAC) and the effect of gas-oxidation treatment on its adsorption performance. New Carbon Materials 2010;25:460–4.

[54]   Liu C, Liang X, Liu X, Wang Q, Teng N, Zhan L, et al. Wettability modification of pitch-based spherical activated carbon by air oxidation and its effects on phenol adsorption. Applied Surface Science 2008;254:2659–65.

[55]   Qin Y, Fan G, Liu K, Hu M. Vanadium pentoxide hierarchical structure networks for high performance ethanol gas sensor with dual working temperature Characteristic. Sensors and Actuators B 2014;190:141–8.

34

[56] Romero-Anaya AJ, Ouzzine M, Lillo-Ródenas MA, Linares-Solano A. Spherical carbons: synthesis, characterization and activation processes. Carbon 2014;68:296-307.

[57] Romero-Anaya AJ, Lillo-Ródenas MA, Salinas-Martínez de Lecea C, Linares-Solano A. Hydrothermal and conventional H_3PO_4 activation of two natural bio-fibers. Carbon 2012;50:3158-69.

[58] Rodríguez-Reinoso F, Linares Solano A. Microporous structure of activated carbons as revealed by adsorption methods. In: Thrower PA, editor. Chemistry and physics of carbon, vol 21. New York: Marcel Dekker; 1988. p. 1–146.

[59] Linares-Solano A, Salinas-Martínez de Lecea C, Alcañiz-Monge J, Cazorla-Amorós D. Further advances in the characterization of Microporous carbons by Physical adsorption of gases. Tanso 1998;185:316-25.

[60] Naono H, Hakuman M, Shimoda M, Nakai K, Kondo S. Separation of Water and Ethanol by the Adsorption Technique: Selective Desorption of Water from Micropores of Active Carbon. Journal of Colloid and Interface Science 1996;182:230-8.

[61] Alcañiz-Monge J, Linares-Solano A, Rand B. Water Adsorption on Activated Carbons: Study of Water Adsorption in Micro- and Mesopores. J. Phys. Chem. B 2001;10: 7998-8006.

[62] Alcañiz-Monge J, Linares-Solano A, Rand B. Mechanism of Adsorption of Water in Carbon Micropores As Revealed by a Study of Activated Carbon Fibers. J. Phys. Chem. B 2002;106:3209-16.

[63] Saidman E, Yurquina A, Rudyk R, Molina MAA, Ferretti FH. A theoretical and experimental study on the solubility, dissolution rate, structure and dipolar

35

moment of flavone in ethanol. Journal of Molecular Structure: Theochem. 2002;585:1-13.

[64]   Boudou JP. Surface chemistry of a viscose-based activated carbon cloth modified by treatment with ammonia and steam. Carbon 2003;41:1955-63.

[65]   Gurvich L. Journal of the Russian Physics and Chemistry Society 1915;47 :805-27.

[66]   Snoeck JW, Froment GF. Steam/CO_2 Reforming of Methane. Carbon Filament Formation by the Boudouard Reaction and Gasification by CO_2, by H_2, and by Steam: Kinetic Study. Ind. Eng. Chem. Res. 2002, 41, 4252-65.

[67]   Zielke U, Hüttinger KJ, Hoffman WP. Surface-oxidized carbon fibers: I. Surface structure and chemistry. Carbon 1996;34:983-98.

[68]   Marchon B, Carrazza J, Heinemann H, Somorjai GA. TPD and XPS studies of O_2, CO_2, and H_2O adsorption on clean polycrystalline graphite. Carbon 1988;26:507-14.